Supporting information

Real-Time Visualization of Cell Membrane Damage using Gadolinium-Schiff Base Complex-Doped Quantum Dots

Amitava Moulick[1,2], Zbynek Heger[1,2], Vedran Milosavljevic[1,2], Lukas Richtera[1,2], Joaquin Barroso-Flores[3], Miguel Angel Merlos Rodrigo[1,2], Hana Buchtelova[1,2], Robert Podgajny[4], David Hynek[1,2], Pavel Kopel[1,2] and Vojtech Adam[1,2]*

[1]Department of Chemistry and Biochemistry, Mendel University in Brno, Zemedelska 1, CZ-613 00 Brno, Czech Republic

[2]Central European Institute of Technology, Brno University of Technology, Purkynova 123, CZ-612 00 Brno, Czech Republic

3Centro Conjunto de Investigación en Química Sustentable UAEM-UNAM, Carretera Toluca–Atlacomulco Km 14.5, Unidad San Cayetano, CP-50200 Toluca, Estado de México

[4]Faculty of Chemistry, Jagiellonian University, Ingardena 3, PL-30060 Krakow, Poland

***Corresponding Author**

Vojtech Adam, Department of Chemistry and Biochemistry, Mendel University in Brno, Zemedelska 1, CZ-613 00 Brno, Czech Republic; E-mail: vojtech.adam@mendelu.cz, Tel.: +420-5-4513-3350; Fax: +420-5-4521-2044

Methods

1. Cell viability assay. The cells were harvested, washed four times with PBS (pH 7.4) and counted using a Countess IIFL automated cell counter (Life Technologies, Carlsbad, CA). The viability of the cells was estimated through the XTT assay. Briefly, a suspension of 5,000 cells in 50 µL of medium was added to each well of a microtiter plate (E-plates 96), followed by incubation at 37°C with 5% CO_2 for 24 h to ensure cell growth. Next, 50 µL of the medium containing the control CdTe QDs or GdQDs was added to each of the wells containing the cells. Final concentrations of 0-100 µM CdTe QDs or GdQDs were used to determine their effect on cell viability. The treated cells were incubated for 24 h using the same conditions described before. Further, 25 µL of the solution containing XTT and phenazine methosulfate was directly added to each of the wells containing the cells, and the mixture was incubated for 2 h at 37°C. The absorbance of the samples was determined at 450 nm (Infinite 200PRO, Tecan).

2. Synthesis of fine fractions of large area graphene oxide (GO). Large area GO was synthesized using chemical oxidation of graphite flakes (5.0 g, 100 mesh, ≥75% min, Sigma-Aldrich) in a mixture of concentrated H_2SO_4 (670 mL, ACS reagent 95.0%–98.0%) and $KMnO_4$ (30.0 g, >99%) according to the simplified Hummer's method[1,2]. The reaction mixture was stirred vigorously. After four days, the oxidation of graphite was terminated by slow adding of H_2O_2 solution (250 mL, 30 *wt* % in H_2O) and the color of the mixture turned to bright yellow, indicating high oxidation level of graphite. The formed graphite oxide was washed three times with 1 M of HCl and washed again several times with deionized water (total volume used 12 L) until a constant pH value (4–5) was achieved. During the washing process with deionized water, the exfoliation of the graphite oxide led to the thickening of the solution and formation of a stable colloid of GO. Very fine isolated GO was subsequently washed several times in Milli-Q water to achieve a constant pH (4–5). For separation of the

fine fraction of GO solution, the centrifugation was used exclusively (25 000 rpm, from 30 to 90 minutes according to the requirement). The purity and composition of the synthesized products were examined using different techniques including SEM (Figure S5, Supporting Information)[3] and AFM (Figure S6, Supporting Information)[4].

3. Details on the NBODel procedure. The NBO Deletion (NBODel) consists in setting to zero –hence deleting– Elements of the Fock Matrix, which correspond to those orbitals or set of orbitals that make up a specific interaction; after deletion, the resulting Fock Matrix is re-diagonalized which generates a new set of eigenvalues and eigenvectors with a concomitant rise energy[5]. The resulting energy difference is ascribed to the absence of the deleted interaction. Herein, the elements deleted were all those common to the full set of orbitals in the alpha and beta density from Gd^{3+} and the rest of the molecule as a mean to estimate the energy with which this cation is bound to the ligand. These so called deletion energies were also calculated under the NBO formalism.

Figures

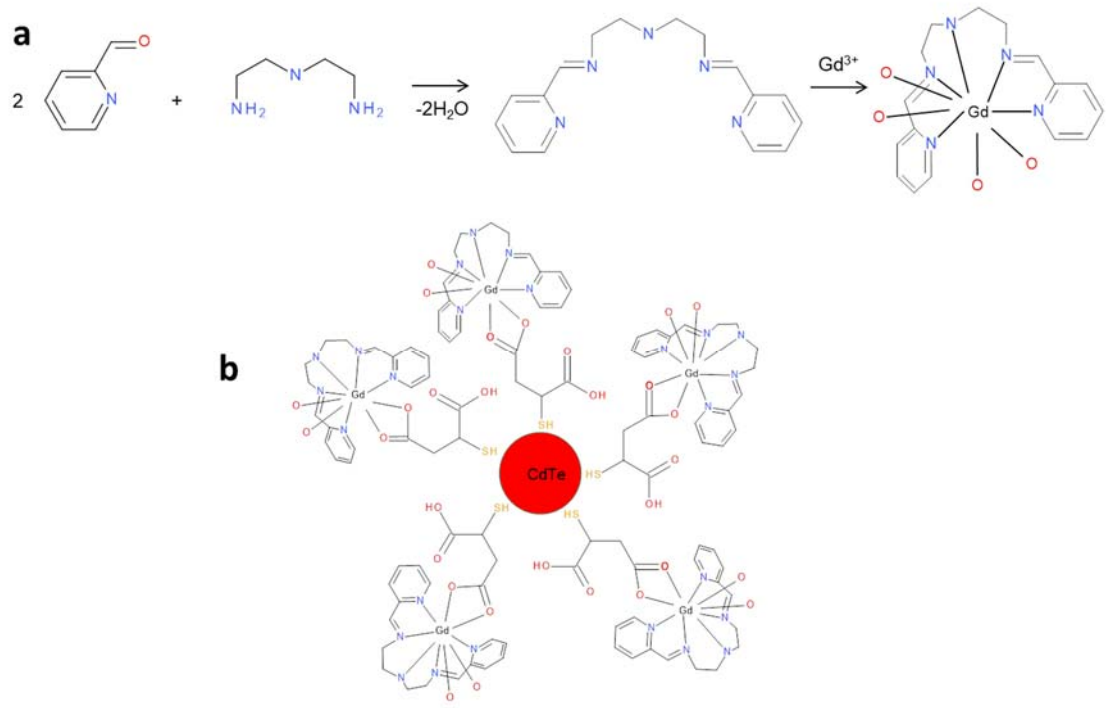

Figure S1: Schematic representation: a) The synthesis of Schiff base [(2-[(E)-2-pyridylmethyleneamino]-N-[2-[(E)-2-pyridylmethylene-amino]ethyl]ethanamine)] and its gadolinium complex. b) The proposed binding of gadolinium complex with CdTe via carboxylate bridges of MSA is shown in lower panel.

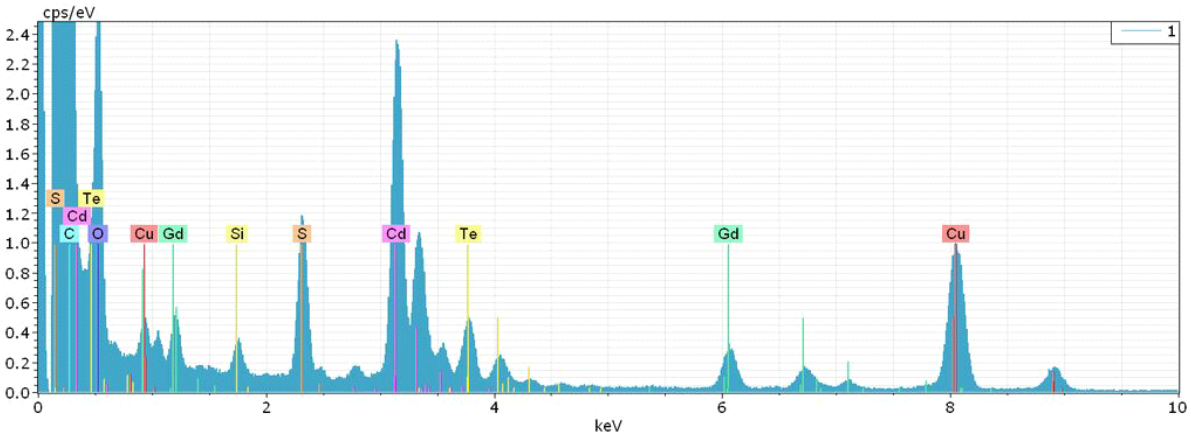

Figure S2. EDX spectrum of GdQDs.

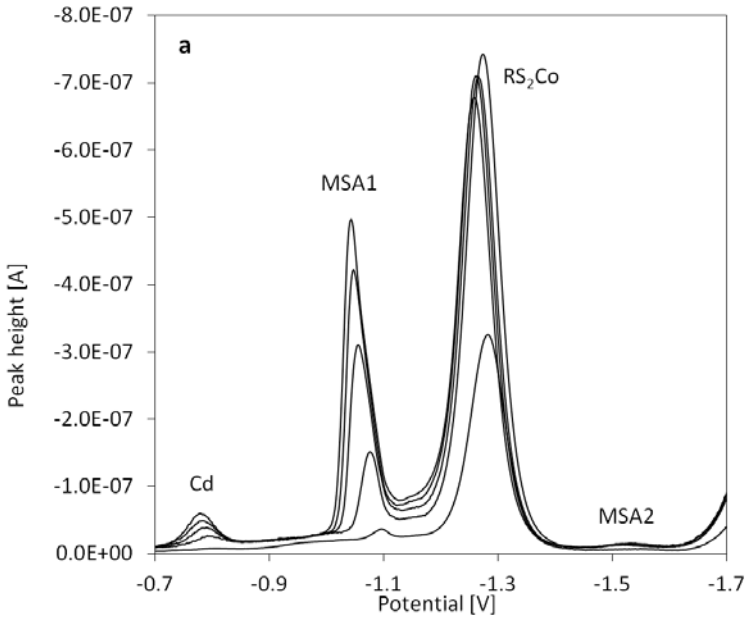

Figure S3. (**a**) Representative differential pulse voltammograms for various concentrations (10; 20; 30; 40 and 50 µM) of CdTe QDs modified with MSA in order of increasing Cd and MSA1 peak heights.

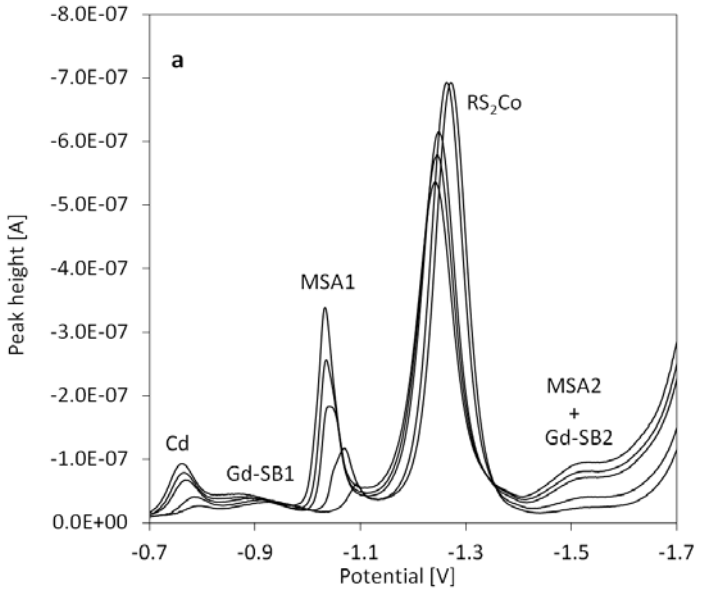

Figure S4. (**a**) Representative differential pulse voltammograms for various concentrations (10; 20; 30; 40 and 50 µM) of GdQDs in order of increasing Cd and MSA1 peak heights.

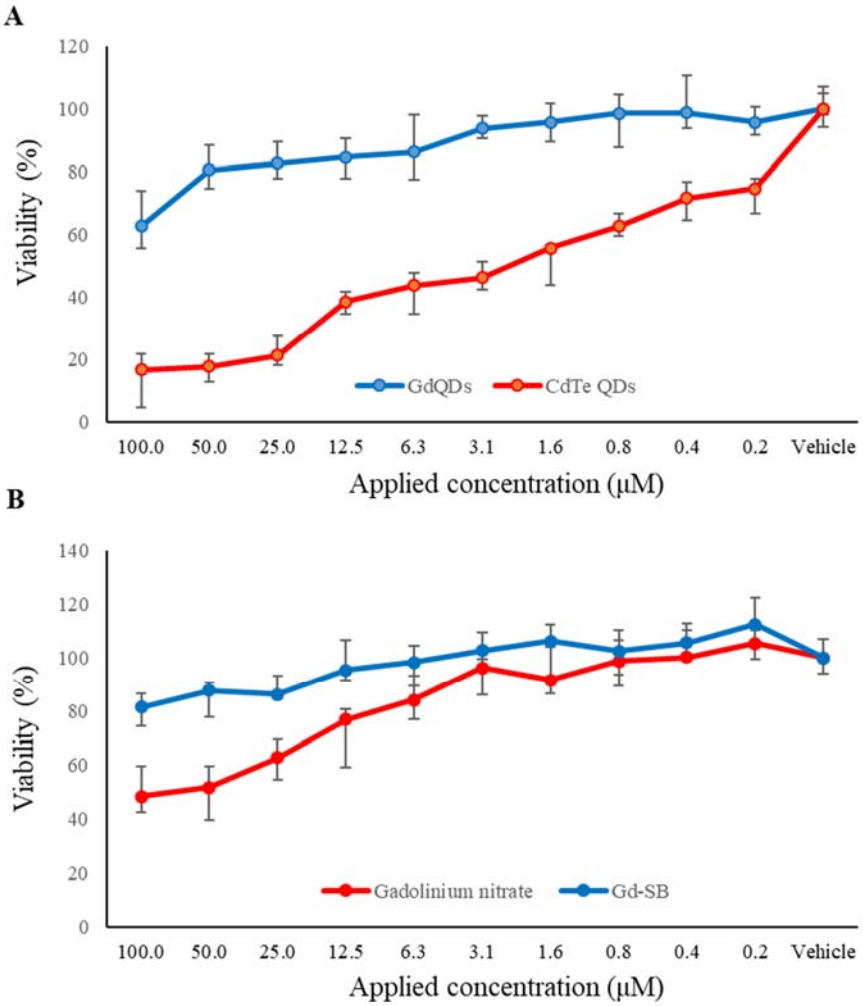

Figure S5. Cytotoxic screening using XTT assay showing: (**A**) comparative analysis of cytotoxicity of CdTe QDs and GdQDs on PC-3 cells and (**B**) cytotoxic screening of gadolinium nitrate and Gd-SB. Vehicle – PBS, pH 7.4. The values are expressed as the mean of six independent replicates ($n = 6$). Vertical bars indicate standard error.

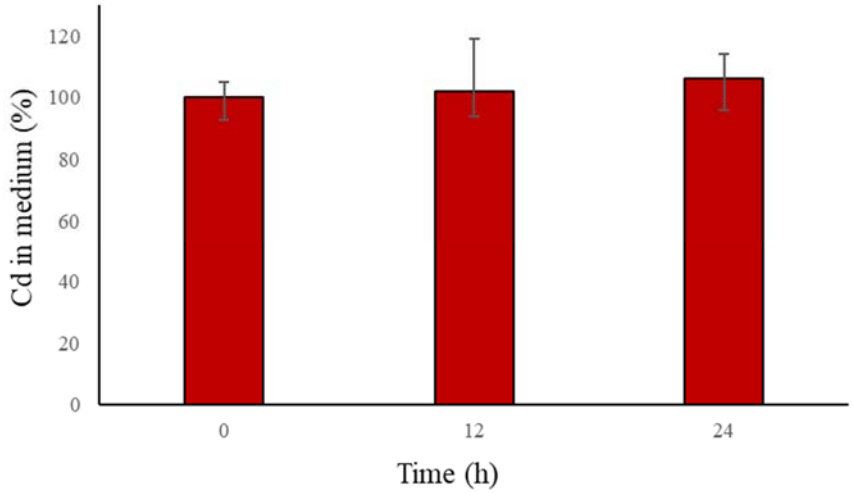

Figure S6: Total Cd released from GdQDs in cell culture medium (RPMI-1640). The GdQDs were mixed with fully supplemented Ham's F12 medium [10% foetal bovine serum, penicillin (100 U/mL) and streptomycin (0.1 mg/mL)] and incubated in 5% CO_2 and 90–100% relative humidity at 37°C in an incubator. Prior to analysis, samples were filtered through 10 kDa Amicon Ultra and digested by microwave-assisted hydrolysis in nitric acid. Finally, the samples were analysed using graphite furnace atomic absorption spectrometer (GFAAS) 280Z AA (Agilent, Santa Clara, CA, USA). Values are expressed as mean of three independent GFAAS analyses. Data represent mean ± standard error, n=6.

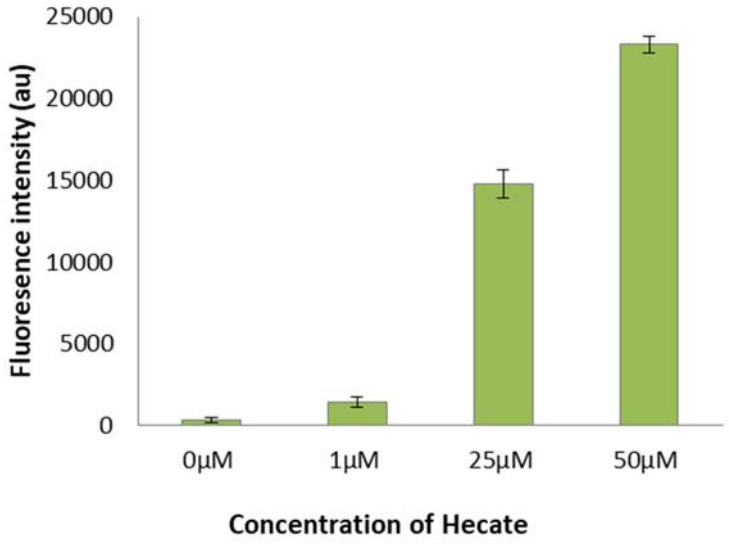

Figure S7: The quantitative correlation between the extent of cell membrane damage and fluorescent intensity of aggregated GdQDs. Different concentration of Hecate was applied to PC3 cell and then the intensity of the GdQDs which were aggregated within the area of damage are measured. Data represent mean ± standard error, n=6.

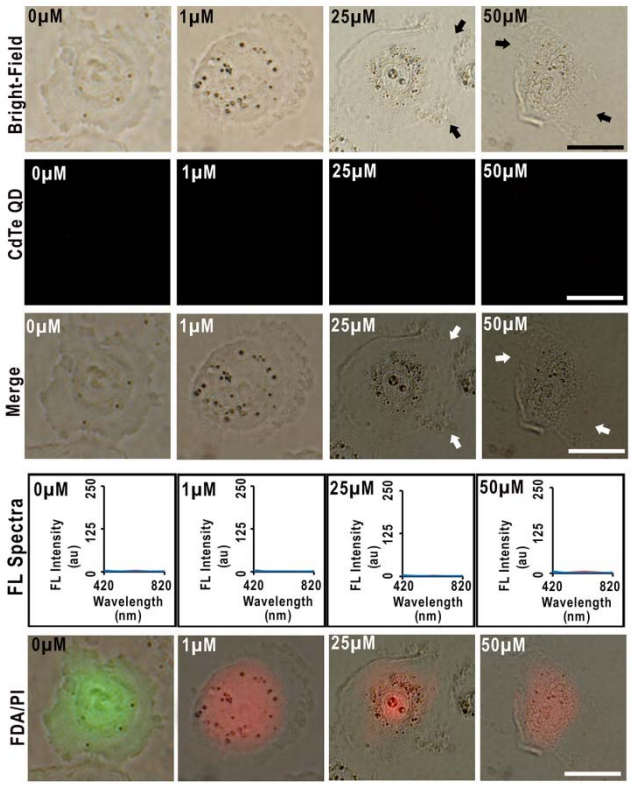

Figure S8: Cells were treated with different concentrations (indicated at the top of each figure) of Hecate to damage the plasma membrane and subsequently stained with CdTeQDs. Pictures of the cells were taken with a fluorescence microscope. Arrows indicate some of the damaged areas of the plasma membrane. The fluorescence spectra of 5,000 Hecate-untreated and -treated cells (stained by CdTeQDs) are shown in the fourth row. The blue and red lines indicate the control (without CdTeQDs staining) and sample (with CdTeQDs staining) cells, respectively. The membrane integrity of the PC-3 cells was assessed by double staining with fluorescein diacetate (FDA, green) and propidium iodide (PI, red). The merged FDA/PI-staining and bright-field images are shown in the fifth row. The length of scale bar is 20 μm.

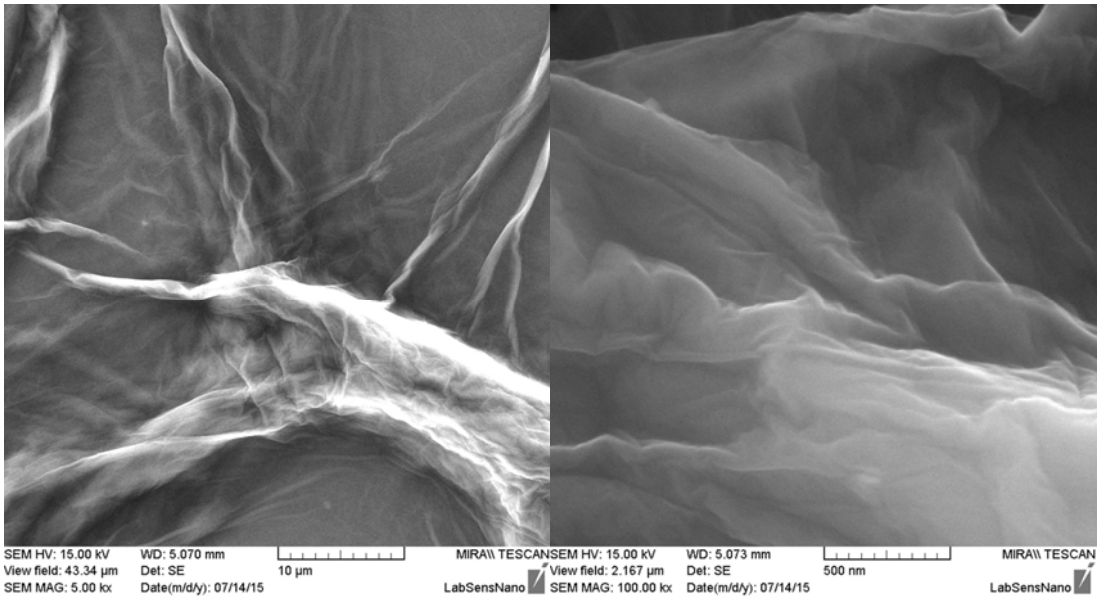

Figure S9. SEM micrographs of GO.

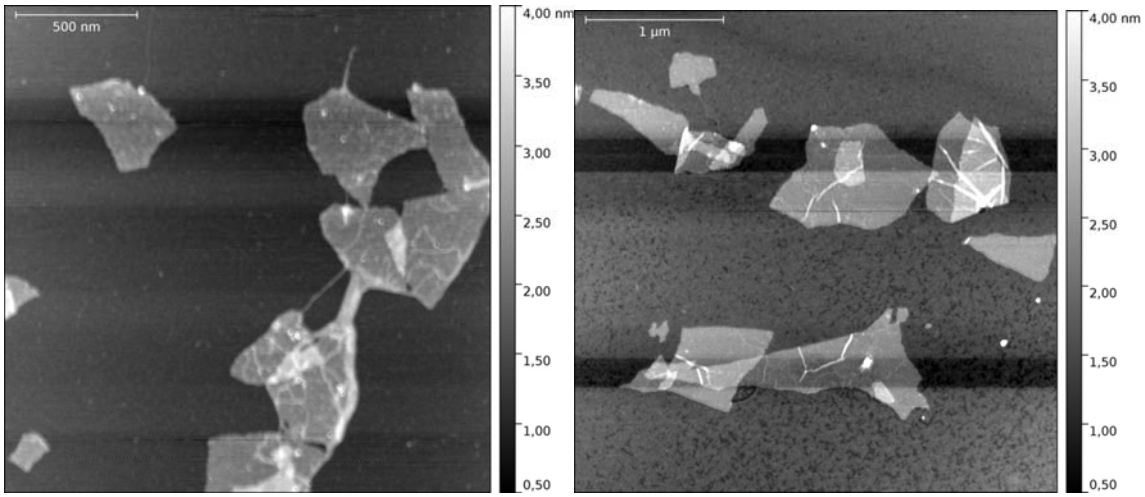

Figure S10. AFM micrographs of GO.

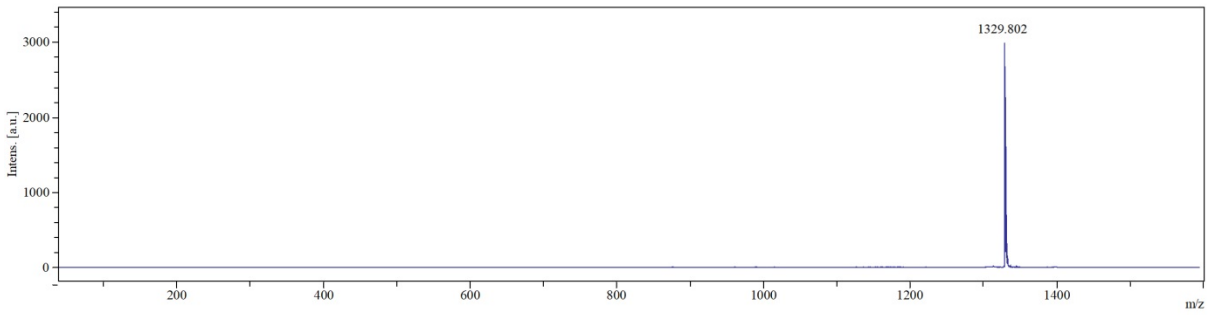

Figure S11. MALDI-TOF spectrum of the synthesized peptide.

References

(1) Hummers, W. S.; Offeman, R. E. Preparation of Graphitic Oxide. *J. Am. Chem. Soc.* **1958,** *80* (6), 1339-1339, DOI: 10.1021/ja01539a017.
(2) Lim, H. N.; Huang, N. M.; Loo, C. H. Facile preparation of graphene-based chitosan films: Enhanced thermal, mechanical and antibacterial properties. *J. Non-Cryst. Solids* **2012,** *358* (3), 525-530, DOI: 10.1016/j.jnoncrysol.2011.11.007.
(3) Richtera, L.; Chudobova, D.; Cihalova, K.; Kremplova, M.; Milosavljevic, V.; Kopel, P.; Blazkova, I.; Hynek, D.; Adam, V.; Kizek, R. The composites of graphene oxide with metal or semimetal nanoparticles and their effect on pathogenic microorganisms. *Materials* **2015,** *8* (6), 2994-3011.
(4) Kudr, J.; Richtera, L.; Nejdl, L.; Xhaxhiu, K.; Vitek, P.; Ruttkay-Nedecky, B.; Hynek, D.; Kopel, P.; Adam, V.; Kizek, R. Improved electrochemical detection of zinc ions using electrode modified with electrochemically reduced graphene oxide. *Materials* **2016,** *9* (1), 1-12.

(5) Weinhold, F. Natural Bond Orbital Methods. In *Encyclopedia of Computational Chemistry*; Schleyer, P. v. R. A., N. L.; Clark, T.; Gasteiger, J.; Kollman, P. A.; Schaefer III, H. F.; Schreiner, P. R., Ed.; John Wiley & Sons: 1998; pp 1792-1811.